Effect of Temperature on Particle Separation in Hollow Fiber Flow Field-Flow Fractionation

Myeong Hee Moon*
Department of Chemistry, Kangnung National University, Kangnung 210-702, Korea

Kyung Hyun Lee, Byung Ryul Min
Department of Chemical Engineering, Yonsei University, Seoul 120-749, Korea

Received 20 March 1999; accepted 30 June 1999

Abstract: Hollow fiber flow field-flow fractionation (HF-FlFFF) has been tested by varying the temperature (21–73°C) to increase separation speed with reduced lift forces. It has been experimentally shown that the separation time of 0.050–0.426-μm polystyrene latex standards can be reduced approximately by half, at 59°C, compared to the separation at room temperature. In addition, the resolution for the separation of large diameter particles, which are often influenced by the lift forces, is greatly improved. It also has been found that the steric inversion diameter can be possibly shifted to a larger diameter (up to about 0.800 μm) at 73°C. The steric retention of particles is observed to increase with temperature due to the decrease in hydrodynamic lift forces that is known to decrease with the viscosity of the carrier liquid. © 1999 John Wiley & Sons, Inc. J Micro Sep 11: 676–681, 1999

Key words: *hollow fiber, hollow fiber flow field-flow fractionation, particle separation, temperature elevation*

INTRODUCTION

Field-flow fractionation (FFF) is a category of separation techniques that fractionate colloidal particles or macromolecules by the use of external fields driven across the direction of separation flow for sample migration [1]. Among the various FFF subtechniques, flow FFF (FlFFF) has been developed into a universal technique for separating and characterizing colloidals and macromolecules [1–5]. Flow FFF utilizes the secondary transverse flow as an external field passing through the permeable walls that consist of ceramic frits. Most FlFFF systems in use adopt a flat rectangular conduit as a channel (column in chromatography) made from a spacer cut in a ribbon shape. The channel is constructed by inserting a spacer between two plastic blocks having permeable frits on both sides (the symmetrical system [2,5]) or only one frit where the crossflow flows out (the asymmetrical system [4,6]). Attempts to facilitate the system operation and to enhance performance, the frit inlet injection method [7–9] or the frit inlet–frit outlet technique [10] have been tried with conventional systems.

However, a cylindrical hollow fiber has been studied as a separation chamber in flow FFF by Lee et al. [11] and followed up with a feasibility study by Jönsson and Carlshaf [12]. A number of works were made with the examination of the ionic strength effect of carrier solution [13] and the properties of fiber membrane on particle separation [14]. Hollow fiber flow FFF (HF-FlFFF) has also been applied to the separation of water soluble polymers and a few protein standards [15]. Recently, it has been reported that particle separation by HF-FlFFF can be greatly improved to the resolution level normally achieved by a rectangular system by optimization [16]. Furthermore, it has been shown that hollow fiber can be a potential alternative to obtain particle size distribution since it can possibly be developed into a disposable module in HF-FlFFF.

The sample migration in a hollow fiber follows the basic principles of FFF theory except that the separation takes place in a cylindrical fiber [Figure 1(a)] instead of a rectangular channel. The average distance of a sample migration pathway from the channel wall (or fiber wall) is dependent on the

---

*Present address: Department of Chemistry, Pusan National University Changjeon-Dong, Pusan 609-735, Korea
Correspondence to: M. H. Moon

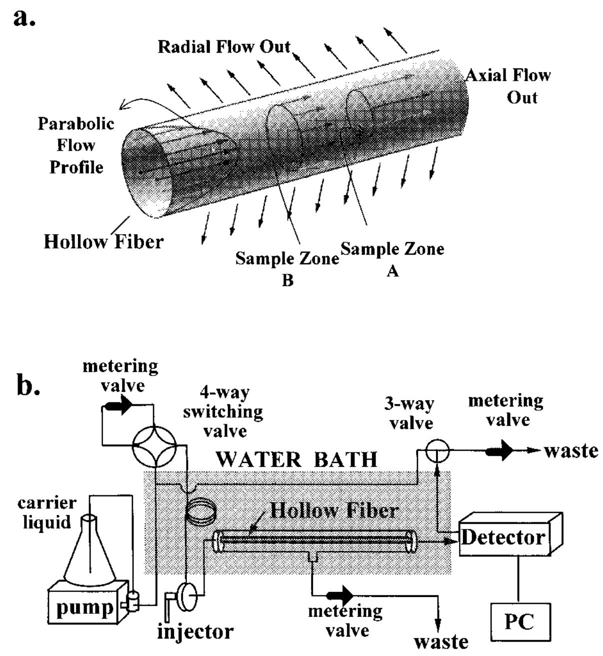

Figure 1. *Schematic view of sample migration in a hollow fiber (a) and the diagram of temperature controlled HF-FlFFF system (b).*

interaction between the applied field (crossflow rate for a rectangular system and radial flow rate for a hollow fiber system) and the opposing diffusive transport of sample materials. Thus in HF-FlFFF, particles or macromolecules having a relatively high diffusion protrude further from the fiber wall and they are eluted earlier than those diffusing slowly, as illustrated in Figure 1(a). (In the figure, sample zones are represented as rings but the actual zone should be a circular band having a gradient in the sample concentration with an exponential decrease toward the fiber wall.) As in other FFF techniques, the retention time in HF-FlFFF is inversely proportional to the diffusion coefficient D [12,16]. The diffusion coefficient is scaled to T/η (η: the viscosity of a carrier liquid) which is reduced with the increase of temperature T. Therefore, elevation of the temperature is a critical factor to increase the diffusion coefficient of sample materials leading to the increase of separation speed.

Temperature elevation has been tried with sedimentation FFF [17] and earlier research has shown that both separation power and speed can be improved experimentally along with theoretical considerations. In addition, the nonequilibrium band broadening, which often occurs in most elution techniques like chromatography including FFF, was reduced [17]. Since the nonequilibrium band broadening is caused by the diffusivity of sample materials located at flow streamlines of unequal flow velocities [18], the elevation of temperature results in the rapid diffusional transport of sample materials among the different flows and it will eventually lead to the decrease in band broadening.

In this study, an HF-FlFFF system has been tested at elevated temperatures to enhance performance with increase of separation speed. Due to the simplicity in constructing a hollow fiber separation module, it is relatively straightforward in terms of establishing a high temperature HF-FlFFF system. Since most flow FFF systems are operated at room temperature, the feasibility of a temperature controlled HF-FlFFF system is significant. By adding temperature control to an HF-FlFFF system, rapid particle separation can be anticipated. It can also be expected that the risk of particle adhesion to the fiber wall may be minimized due to the elevated migration of sample materials from the fiber wall. Decrease of the lift forces can be another advantage in operating the system at an elevated temperature. It was reported in an earlier work [19] that the hydrodynamic lift forces are linearly proportional to the viscosity carrier liquid for a limited range of temperatures. Therefore, the decrease of lift forces will extend the normal operation and it may expand the dynamic range of particle separation in HF-FlFFF. It is likely that the steric inversion diameter can be shifted to a large diameter scale if the lift forces are efficiently suppressed by temperature elevation.

Calculation of the inversion diameter d_i in HF-FlFFF. The retention ratio, R, in the normal mode of HF-FlFFF can be expressed in a limited form by [16]

$$R = \frac{t^0}{t_r} \cong 4\lambda \quad \text{(when } \lambda \ll 0.02 \text{ for HF-FlFFF, at normal mode)}, \tag{1}$$

where t^0 is the void time, t_r is the retention time, and λ in HF-FlFFF is a dimensionless parameter that represents the inverse of the Péclet number Pe:

$$\lambda = \frac{1}{\mathrm{Pe}} = \frac{D}{Ur_f} \quad \left(\text{where } D = \frac{kT}{3\pi\eta d}\right) \tag{2}$$

In Equation (2), U is the radial flow velocity at the fiber wall and r_f is the radius of the fiber. Retention time, t_r, in HF-FlFFF can be written as [12,16]

$$t_r = \frac{r_f^2}{8D} \ln \frac{\dot{V}_{\mathrm{in}} - (L_0/L)\dot{V}_{\mathrm{rad}}}{\dot{V}_{\mathrm{out}}} \tag{3}$$

where $\dot{V}_{\mathrm{in}}$ represents the inlet flow rate, $\dot{V}_{\mathrm{rad}}$ the radial flow rate ($= U2\pi r_f L$), $\dot{V}_{\mathrm{out}}$ the outgoing flow rate at the fiber outlet ($= \dot{V}_{\mathrm{in}} - \dot{V}_{\mathrm{rad}}$), L_0 the point where focusing/relaxation of sample materials is accomplished, and L is the length of a fiber.

Considering the retention ratio of the steric mode only, it can simply be expressed as

$$R = \frac{t^0}{t_r} = 4\gamma\frac{a}{r_f} \quad \text{(at steric mode)} \tag{4}$$

where γ is the steric correction factor that can be found by a calibration procedure and a is the particle radius. Equation (4) is simple modification from the retention ratio for a conventional rectangular FFF system, $R = 6\gamma a/w$ (w: channel thickness), since R for the normal mode of HF-FlFFF is expressed as $R = 4\lambda$ [16] instead of $R = 6\lambda$. Due to the theoretical incompleteness in resolving the retention mechanism of the steric mode, one can utilize the simple relationship of retention time with particle diameter by using the calibration procedure [20,21] as

$$\log t_r = \log t_{r1} - S \log d \tag{5}$$

where t_{r1} is the constant equal to the extrapolated value of t_r for particles of unit diameter and S is the selectivity, the slope of a calibration curve.

When the retention ratio in HF-FlFFF is considered generally, it can be written as the sum of two terms [Equations (1) and (4)] as

$$R = 4\lambda + 2\gamma\frac{d}{r_f} \tag{6}$$

Substitution of Equations (2) and (5) in conjunction with Equation (4) into Equation (6) gives a semi-empirical expression for R with all measurable parameters:

$$R = \frac{t^0}{t_r} = \frac{4kT}{3\pi\eta U r_f d} + \frac{t^0}{t_{r1}} d^S \tag{7}$$

The steric inversion diameter d_i is defined in an earlier work as the diameter for which $\partial R/\partial d = 0$ [20]. Thus, differentiation of Equation (7) followed by the rearrangement of d_i is as follows:

$$d_i = \left(\frac{4kt_{r1}}{3\pi r_f U S t^0} \frac{T}{\eta} \right)^{1/(1+S)} \tag{8}$$

Equation (8) suggests that the inversion diameter for a given flow rate condition is scaled to the $1/(1 + S)$ power of T/η. Therefore, the temperature elevation will induce an increase in inversion diameter. In addition, the inversion diameter is also influenced by the variation of the diameter selectivity S of a calibration curve. The typical selectivity values are approximately 1.5 for steric/hyperlayer runs in flow FFF [21] whereas it is 0.7–0.8 for sedimentation/steric FFF runs [20]. This could be one reason that the steric inversion in flow FFF systems is often observed at a smaller diameter than in sedimentation FFF (normally around 1.0 μm).

MATERIALS AND METHODS

The HF-FlFFF system is identical to the one utilized in previous research [16] except that the hollow fiber separation module is inserted in a water bath as shown in Figure 1(b). A 2-m long coiled Teflon tube (i.d. 0.030 in) is placed right before the injector and immersed in the bath in order to provide rapid elevation of temperature for carrier solution during the delivery. System operation is begun after 2 h of preheating at a desired temperature in the bath. The hollow fiber used is polysulfone, having a molecular weight cutoff of 30,000, obtained from SK Chemicals (Seoul, Korea). The hollow fiber separation module is prepared the same way as described in Reference 16. The dimensions of the fiber are 24.0 cm in length L and 0.40 mm (in dried condition) with radius r_f. The actual value of fiber radius is calibrated to be 0.46 mm by using Equation (3) from an experimental retention time of standard beads obtained at room temperature since fiber expansion occurs during run due to the system pressure [16]. Carrier solution utilized throughout the work is prepared from ultrapure water added with 0.1% FL-70 from Fisher Scientific Co. (Fair Lawn, NJ, USA) for particle dispersion and with 0.02% NaN_3 as a bactericide. Delivery of the carrier solution to hollow fiber is accomplished by a model M930 HPLC pump from Younglin Instrument (Seoul, Korea). Sample injection is made at a reduced flow rate (0.5 mL/min.) through the inlet of the fiber with the use of a Rheodyne 7125 loop injector from Rheodyne (Cotati, CA, USA). Following the sample injection, the focusing/relaxation process is carried out by delivering the carrier liquid into both the inlet and outlet. The focusing/relaxation of injected sample components is made at the position of 0.1 L by adjusting the ratio of inlet and outlet flow rates as 1:9 for a period of time to assure sufficient relaxation as given in the literature [12]. Since the current HF-FlFFF system utilizes a single pump, the flow conversion during the focusing/relaxation process is made by using both four-way and three-way switching valves as depicted in Figure 1(b). Flow rates required for focusing/relaxation are adjusted with a model SS-SS2-VH Nupro metering valve from Nupro Co. (Willoughby, OH, USA). The sample particles used are polystyrene latex standards having nominal diameters of 0.050, 0.096, 0.135, 0.204, 0.304, 0.426, 0.596, 0.806, 1.034, 2.013, and 3.004 μm from Duke Scientific Co. (Palo Alto, CA, USA). Injection amount of standard particles is about 2–3 μL of each diluted sample solution (about 0.1% solid). Eluted particles are monitored by a Model 720 UV detector from Younglin Instrument at a wavelength of 254 nm. The fractogram signal is transferred to a PC by using the Autochro-Win data collection software from Younglin Instrument.

RESULTS AND DISCUSSION

Figure 2 shows the separation of polystyrene latex mixtures obtained at four different temperature conditions (from 23–71°C) by HF-FlFFF. All runs are made at $\dot{V}_{\text{out}}/\dot{V}_{\text{rad}} = 1.42/0.15$ in actual flow rates. At room temperature (23°C), resolution between peaks appears to be excellent up to 0.204 μm but the separation of 0.304- and 0.426-μm particles is not completely achieved at the baseline level. When the temperature is elevated to 51°C, the last two peaks are clearly separated with the simultaneous reduction of retention times for all components. It seems that the resolution between the first two peaks is somewhat decreased. This is due to the increase of the experimental retention ratio which results in the increase of nonequilibrium band broadening in FFF. If the experimental retention ratio is kept constant, in which the radial flow rate is varied inversely with the change in D, the net effect of temperature elevation can be observed with the decrease of nonequilibrium band broadening. However, the current experiment is focused on the enhancement of separation speed and the minimization of steric influences. The baseline separation of the mixture is maintained at 59°C but is destroyed at 71°C. The separation time at 59°C is almost reduced to half without seriously losing the resolution and it is roughly 2.8 times faster at 71°C than that obtained at 23°C. This observation is similar to the earlier result made with a sedimentation FFF system [17]. From the observed fractograms in Figure 2, it is clearly shown that the steric influence on the elution of 426-nm particles is significantly reduced at a high temperature. If there is no steric influence on the separation, retention time of 426-nm particles in Figure 1(a) should be about 1.4 times that of 304-nm standard beads since the retention time is linearly proportional to the particle diameter.

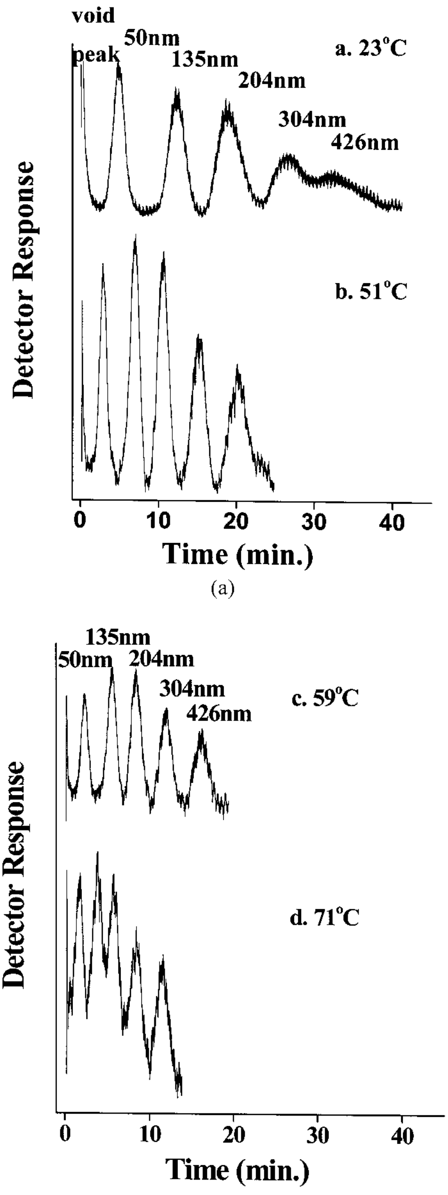

(a)

(b)

Figure 2. *(a)–(d) Fractograms of polystyrene separation by HF-FlFFF obtained at four different temperature conditions. All runs are obtained at the same flow rate condition ((*$\dot{V}_{out}$ */* $\dot{V}_{rad}$ *= 1.42 / 0.15 in actual flow rates).*

The decrease in retention time upon the variation of temperature is plotted in Figure 3(a). Experimental data points are obtained at a run condition of $\dot{V}_{\text{out}}/\dot{V}_{\text{rad}} = 1.41/0.10$ in mL/min. and they are compared with theory (dotted lines) by using Equation (3). These results indicate that the experimental data agree well with theory. It is likely that the fiber expansion from temperature elevation does not seriously occur in the current experiment. Experimental

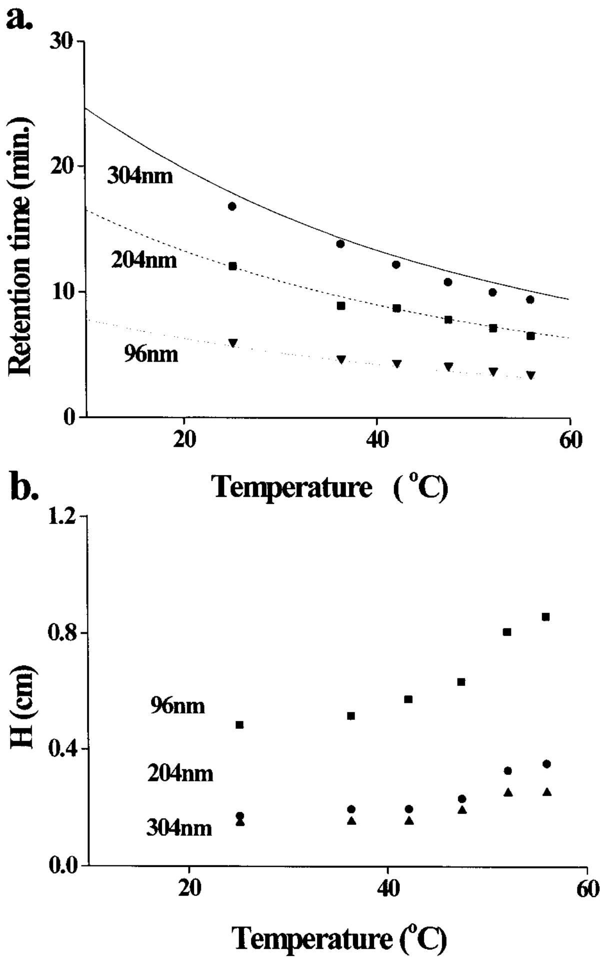

Figure 3. *(a) Plots of experimental retention time at various temperature conditions along with theoretical curves and (b) the measured plate heights vs. temperature. Run condition is $\dot{V}_{out}$ / $\dot{V}_{rad}$ = 1.41 / 0.10 in mL / min.*

plate height data are plotted against temperature in Figure 3(b). Measured plate height does not appear to vary significantly until 42°C for both 204- and 304-nm beads but it increases more than 60% above 52°C. Since the data show plate heights measured at fixed flow rate conditions only, it is not quite clear to determine the evidence of the decrease in nonequilibrium band broadening. However, the current observations imply that contribution of nonequilibrium band broadening to observed plate heights is substantially decreased when operating temperature increases. Otherwise, the observed plate height data will appear to increase with temperature significantly since experimental retention ratio increases as temperature increases.

The steric influence was further examined with a series of latex spheres in Figure 4. The retention

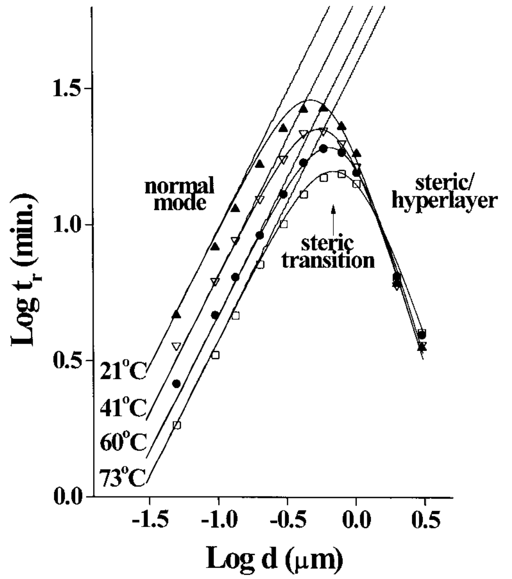

Figure 4. *Plot of log t_r vs. log d for 11 sized standard particles obtained at four different temperature conditions. The straight lines shown at the left side represent the theoretical retention times of the normal mode only at each temperature. The experimental condition for all runs is identical to the one used in Figure 2.*

time of larger diameter standards is measured at elevated temperature conditions and the experimental data are plotted against the particle diameter for 11 different sizes in a logarithmic scale. The straight lines represent the theoretical retention time for normal mode only by using Equation (3). By comparing the retention time of 0.304-μm particles (the fifth point from the left of the figure at each temperature condition), deviation from the theory (the straight lines) appears to decrease as the temperature increases. This shows that the steric effect does not dominate in the elution of these particles. Since the hydrodynamic lift forces found by experiments has been known to increase with the viscosity of a carrier liquid [19], temperature elevation causes a decrease of viscosity which in turn results in the decrease of the lift forces. At 21°C, the steric inversion appears between 0.426 and 0.596 μm. As the temperature increases, the inversion diameter (the maximum point of the curve) shifts to nearly 0.8 μm at 73°C which implies that the temperature elevation results in the extension of inversion diameter to a large diameter scale. Calculation of an accurate inversion diameter is not carried out for the data sets used in this work since the number of data points available for the steric calibration was insufficient to obtain appropriate calibration parameters

(S and t_{r1}) which could cover a wide diameter range in the steric regime (the right hand side of the curve maxima in the figure). For this reason, steric calibration could not be established and a generalized retention time curve covering the normal, steric transition, and steric region is not plotted in Figure 4 (the curves in Figure 4 are the best fit drawing). However, the increase in inversion diameter observed in Figure 4 is consistent with theoretical expectations explained in Equation (8). In addition, it demonstrates that temperature elevation can be an alternative method to expand the dynamic range of particle separation in HF-FlFFF.

It is remarkable that the retention time of steric particles (2.013 and 3.044 μm) in Figure 4 increases as the temperature increases. This phenomenon is the reverse of that observed in the normal mode. The conversion of elution order begins to appear with 2.013-μm particles and it shows clearly with 3.004-μm particles in which the retention time increases with the increase of the temperature. The unusual increase of steric retention of particles can also be explained by the decrease of the hydrodynamic lift forces at the elevation of temperature. Therefore, at higher operating temperatures the particles are positioned closer to the fiber wall due to the reduced lift forces at a lower solution viscosity. This explanation is not clearly supported with detailed experiments at the steric regime in this research. However, an earlier work supports that steric retention of particles is greatly reduced when the viscosity of the carrier solution is increased by using a ternary mixture [19].

ACKNOWLEDGMENT

BRM is grateful for financial support from the Korea Science and Engineering Foundation (KOSEF 95-0502-01-3). The authors thank SK Chemicals (Seoul, Korea) for providing the hollow fibers.

REFERENCES

1. Giddings, J. C. Science, 1993, 260, 1456.
2. Caldwell, K. D. Anal Chem 1988, 60, 959A.
3. Ratanathanawongs, S. K.; Giddings, J. C. Chromatography of Polymers: Characterization by SEC and FFF, Provder, T., Ed., ACS Symp. Series 521, ACS, Washington, DC, 1993.
4. Wittgren, B.; Wahlund, K.-G.; Derand, H.; Wesslen, B. Macromolecules, 1996, 29, 268.
5. Moon, M. H.; Kim, Y. H.; Park, I. J Chromatogr 1998, 813, 91.
6. Litzen, A; Wahlund, K.-G. J Chromatogr 1989, 476, 413.
7. Liu, M.-K.; Williams, P. S.; Myers, M. N.; Giddings, J. C. Anal Chem 1991, 63, 2115.
8. Moon, M. H.; Kwon, H.; Park, I. Anal Chem 1997, 69, 1436.
9. Moon, M. H.; Kwon, H.; Park, I. J Liq Chrom & Rel Technol 1997, 20, 2803.
10. Li, P.; Hansen, M.; Giddings, J. C. J Microcol Sep 1998, 10, 7.
11. Lee, H.-L; Reis, J. F. G.; Dohner, J.; Lightfoot, E. N. AIChE J 1974, 20, 776.
12. Jönsson, J. A.; Carlshaf, A. Anal Chem 1989, 61, 11.
13. Jönsson, J. A.; Carlshaf, A. J Microcol Sep 1991, 3, 411.
14. Carlshaf, A.; Jönsson, J. A. Sep Sci Technol 1993, 28, 1031.
15. Wijnhoven, J. E. G. J.; Koorn, J.-P.; Pope, H.; Kok, W. Th. J Chromatogr 1996, 732, 307.
16. Lee, W. J.; Min, B.-R.; Moon, M. H. Anal Chem 1999, 71, 3446.
17. Giddings, J. C.; Xu, Y.; Marcus, M. N. Anal Chem 1994, 66, 3047.
18. Giddings, J. C. Unified Separation Science Wiley: New York, 1991.
19. Williams, P. S.; Moon, M. H.; Xu, Y.; Giddings, J. C. Chem Eng Sci 1996, 51, 4477.
20. Moon, M. H.; Giddings, J. C. Anal Chem 1992, 64, 3029.
21. Barman, B. N.; Ashwood, E. R.; Giddings, J. C. Anal Biochem 1993, 212, 35.